
Princeton Plasma Physics Laboratory

PPPL-

PPPL-



Prepared for the U.S. Department of Energy under Contract DE-AC02-76CH03073.

Princeton Plasma Physics Laboratory

Report Disclaimers

Full Legal Disclaimer

This report was prepared as an account of work sponsored by an agency of the United States Government. Neither the United States Government nor any agency thereof, nor any of their employees, nor any of their contractors, subcontractors or their employees, makes any warranty, express or implied, or assumes any legal liability or responsibility for the accuracy, completeness, or any third party's use or the results of such use of any information, apparatus, product, or process disclosed, or represents that its use would not infringe privately owned rights. Reference herein to any specific commercial product, process, or service by trade name, trademark, manufacturer, or otherwise, does not necessarily constitute or imply its endorsement, recommendation, or favoring by the United States Government or any agency thereof or its contractors or subcontractors. The views and opinions of authors expressed herein do not necessarily state or reflect those of the United States Government or any agency thereof.

Trademark Disclaimer

Reference herein to any specific commercial product, process, or service by trade name, trademark, manufacturer, or otherwise, does not necessarily constitute or imply its endorsement, recommendation, or favoring by the United States Government or any agency thereof or its contractors or subcontractors.

PPPL Report Availability

Princeton Plasma Physics Laboratory:

<http://www.pppl.gov/techreports.cfm>

Office of Scientific and Technical Information (OSTI):

<http://www.osti.gov/bridge>

Related Links:

[U.S. Department of Energy](#)

[Office of Scientific and Technical Information](#)

[Fusion Links](#)

Deuterium Retention in NSTX with Lithium Conditioning

C.H. Skinner^a, J.P. Allain^b, W. Blanchard^a, H.W. Kugel^a, R. Maingi^c,
L. Roquemore^a, V. Soukhanovskii^c, C.N. Taylor^b.

^a*Princeton Plasma Physics Laboratory, Princeton NJ, 08543 USA.*

^b*Purdue University, West Lafayette, 400 Central Drive, IN 47907, USA.*

^c*Oak Ridge National Laboratory, Oak Ridge TN 37831, USA.*

^d*Lawrence Livermore National Laboratory, Livermore, CA 94551 USA.*

Abstract:

High ($\approx 90\%$) deuterium retention was observed in NSTX gas balance measurements both with and without lithiumization of the carbon plasma facing components. The gas retained in ohmic discharges was measured by comparing the vessel pressure rise after a discharge to that of a gas-only pulse with the pumping valves closed. For neutral beam heated discharges the gas input and gas pumped by the NB cryopanel were tracked. The discharges were followed by outgassing of deuterium that reduced the retention. The relationship between retention and surface chemistry was explored with a new plasma-material interface probe connected to an in-vacuo surface science station that exposed four material samples to the plasma. XPS and TDS analysis showed that the binding of D atoms is fundamentally changed by lithium – in particular atoms are weakly bonded in regions near lithium atoms bound to either oxygen or the carbon matrix.

PSI keywords: Deuterium Retention, Lithium, NSTX.

JNM keywords: P0500 Plasma-Materials Interaction, L0300 Lithium, S1300 Surface Effects, R0900 Redeposition.

PACS codes: 52.40.Hf Plasma-material interactions; boundary layer effects,
52.90.+z Other topics in physics of plasmas and electric discharges

Corresponding and presenting author address:

Charles H. Skinner, Princeton Plasma Physics Laboratory, POB 451, Princeton NJ 08543 USA.

Email: cskinner@pppl.gov, Phone: 609 243 2214, Fax: 609 243 2665

1. Introduction

Fuel retention is an important constraint in the selection of plasma facing materials for next-step tokamaks. Ever since the first observations of co-deposition on JET[1] and TFTR[2] tiles extensive gas-balance and material analysis measurements of retention in tokamaks have been carried out and were recently reviewed by Loarer[3]. Short term retention (dynamic retention) is closely linked to implantation of the recycling flux and was identified in Asdex-U, DIII-D, JET, NSTX and Tore Supra[4,5,6,7]. Basic parameters of hydrogenic retention in ITER's plasma facing materials were discussed in ref. [8].

Lithiumization of carbon plasma facing components led to substantial advances in plasma performance in TFTR[9]. These were followed up in subsequent experiments with a liquid lithium capillary pore system at T11-M[10], FTU[11], with a liquid lithium tray in CDX-U[12] and with lithiumization of the TJ-II stellarator[13]. A new full liquid lithium thin-film wall tokamak (LTX) will begin operation in 2010[14]. Lithiumization of the National Spherical Torus Experiment NSTX has shown beneficial effects such as improved confinement and reduction and elimination of ELMs[15,16]. A liquid lithium divertor[17] has been installed to explore divertor pumping over a large area with a view to future high flux-expansion solutions for power exhaust and the attainment of the Li-wall regime[18].

Lithium is known to have a high chemical affinity for hydrogen and retention of deuterium in lithium can occur up to an atomic ratio of 1:1 [19]. Laboratory experiments have shown a strong reduction in the physical [20,21] and chemical [22] sputtering of graphite after deposition of lithium. Chemical bonding states of lithium on a graphite surface were explored in particle beam laboratory experiments in ref. [21]. In this paper we report on gas balance measurements of deuterium retention in NSTX both before and with lithium conditioning of its graphite walls. Insights into deuterium retention of lithiated graphite were obtained from surface analysis of samples exposed with a new PMI probe in the outer divertor connected *in-vacuo* to a surface science station with thermal desorption spectroscopy (TDS). Related work on surface chemistry of NSTX tiles is reported in refs. [21,23,24].

2. Gas balance measurements.

The difference between fueling and exhaust is commonly used to measure short term variations in the wall hydrogenic inventory in tokamaks. In support of gas balance measurements on NSTX a new high accuracy baratron (MKS 690A) with calibration traceable to a NIST standard was installed and calibrations of all the vessel ionization gauges, fast microion gauges (5ms response) and residual gas analyzers were performed over the 1e-6 to 1e-3 torr range for both nitrogen and deuterium. The small ($\sim 6\%$) effect of the TF field on the in-vessel microion gauges was measured. The gas injectors, the small amount of fueling by cold deuterium that is an intrinsic part of neutral beam (NB) operation, and the NB cryopumping speed were all measured separately.

Baseline ohmic and NB heated discharges were developed with the outer strike point on the outer divertor at $R=0.75 - 0.85$ m, close to the PMI probe at $R=1.042$. The ramp down in plasma current was carefully programmed to avoid a minor disruption that would heat the tiles and possibly influence the retention. Intershot He-GDC for 8-9 minutes was used before lithiumization, but not used (was unnecessary) with lithium conditioning. For ohmic discharges all the pumping valves were closed and the retention measured by comparing the vessel pressure after the discharge to the pressure rise with the same gas pulse but without initiating a plasma. This method avoids any uncertainty in plenum and vessel volumes. Fig. 1 shows results from an ohmic discharge with lithium conditioning. The retention, R , after the ohmic discharge was estimated from eq. 1 where P_d , P_g is the pressure immediately following discharge termination and F_d , F_g the deuterium fueled, with the subscripts referring to the discharge and gas-only cases:

$$R = 1 - \left(P_d / P_g \times F_g / F_d \right) \quad (1)$$

The deuterium input was programmed to be the same for gas-only and plasma discharge so the measured (F_g/F_d) is close to one. The retention for 133014 (Fig. 1) is 94.3%. This may be compared to the pre-lithium retention in 132489 of 92.8%. The gas fueling for these discharges was similar: 29.3 torr-liters for 132489, 23.3 torr-liters for 133014. The calculated retention was quite reproducible (within 1%) in a sequence of nominally identical discharges, indicating that the small $\sim 2\%$ difference between the average of pre-Li (92%) and with-Li discharges (94%) is significant and attributable to lithium. However discharges with fluctuations in the stored energy,

or a tail end disruption showed lower retention (e.g. 133017: 87%). These were excluded from the averaging.

The retention rate can also be expressed as a function of ion fluence to the wall. The total ion fluence (particles) incident on the outer divertor was derived from combining ion saturation current measurements by the two Langmuir probes on the outer divertor with the D-alpha emission profile. For the ohmic pre-lithium discharge 132489 this was 2.4×10^{22} D ions and for the ohmic with-lithium discharge 133014 this was 2.65×10^{22} D ions. The deuterium retention measured by gas balance on this pair of discharges was 1.9×10^{21} and 1.5×10^{21} D atoms, which corresponds to 8% and 6% of the outer divertor ion fluence. This does not include D flux to the inner divertor, the center stack or outer vessel wall[25] so the number for the retention rate as a function of the total ion fluence to the wall and divertor will be less.

Retention in discharges heated by neutral beams was measured by tracking the balance between input and exhausted deuterium. The pre-Li discharges were ELMy H-mode. The post-lithium discharges were mostly ELM-free H-mode. The lithium reduced the density, increased the temperature, and stored energy in most cases, by 20-30%. A comparison of the in-vessel pressure during the discharge to that of a similar gas-only 'shot' is shown in Fig. 2 and indicates that there is high retention in these discharges. The pressure variation after the discharge is due to cryopumping by the NB box, residual gas injection from the centerstack gas injector and wall outgassing.

The retention was calculated from the ratio of the wall inventory (total fueling, F_t less deuterium pumped, D_c and deuterium gas remaining in vessel, D_v) to the total fueling, all measured immediately after discharge termination:

$$R = (F_t - D_c - D_v) / F_t \quad (2)$$

The different methodologies of equation 1 and equation 2 were checked against each other by measuring the retention of similar ohmic discharges (pre-Li) both ways i.e. in one case with the NB valve closed and in two discharges with the NB valve open. These discharges had similar plasma current, stored energy and in-vessel pressure during the discharge. The retention calculated by equation 2 was $R = 89.5\%$ and $R = 90.0\%$ in the NB valve open cases and for comparison, the average value calculated by equation 1 was $R = 92.0\%$ for the valves closed

case. This close agreement validates the comparison of retention as measured by the two methods. A summary of the retention results is given in Table 1. Note that the difference with lithium increases with the amount of lithium evaporated. This result is corroborated with laboratory XPS data that identified a minimum lithium thickness required for effective D pumping [24].

Retention	Before Li	With Li
Ohmic	92%	94% (48 mg Li)
NB heated	87%	93% (137 mg Li)

Table 4.1. Retention measured immediately following ohmic and NB heated discharges averaged over 3-8 discharges.

The lithium conditioning induced a substantial decrease in the in-vessel pressure during the discharge. Fig. 3 shows a comparison of a NB heated discharges before- and with lithium conditioning. The gas fueling during the plasma for this pair of discharges was similar: 37 torr-liters for 132474, 41 torr-liters for 133110. With lithium the in-vessel pressure decreases to 40% of the value before Li but interestingly, recovers to the same value after the pulse.

A dynamic particle balance model was used to study the wall pumping and outgassing during the discharge[26,27]. The model takes into account all measured particle sources, such as gas injection, NB injection and the dynamic change in particle inventory, and calculates the wall loading rate. At present, the model used electron inventory as a proxy for plasma particle content, and does not take into account electron contributions from carbon impurities. The wall was found to be in a pumping state throughout nearly all of the analyzed discharges. A significant increase was found in the cumulative wall inventory in lithium conditioned NB heated discharges as shown in fig. 3 panel (d).

Deuterium outgassing follows an NSTX discharge and reduces the retention (TFTR tiles are still outgassing tritium 13 years after the end of plasma operations). The amount of outgassing

increases with lithiumization as the intershot He-GDC is discontinued. Multi-day tracking of the deuterium partial pressure after discharges showed evidence of wall pumping of molecular deuterium. With the pumping valves closed the deuterium pressure rose and reached a plateau of 4.2×10^{-4} torr at 10 h after with-Li plasma operations, but then the pressure then decreased slightly to 4.0×10^{-4} torr at 26 h as the vessel continued to cool.

3. Surface analysis.

To gain insights into the fundamental surface chemistry behind the retention results a 1.2-m linear translator was used to introduce four material samples into a gap between tiles in the NSTX lower outer divertor at a major radius of 1.04 m, with the sample surfaces flush with the surrounding tiles (Fig. 4). After exposure to 6 or 8 nominally identical discharges the samples were withdrawn the same evening for thermal desorption spectroscopy (TDS) in an *in-vacuo* surface science station beneath the NSTX vessel, and then extracted under argon for TDS, SEM and X-ray Photo-electron (XPS) analysis at Purdue University Omicron facility. Prompt sample analysis is important as lithium is chemically active.

Deuterium alone does not have enough electrons to produce an XPS spectrum however indirect interactions of deuterium with O, C and Li are measured and correlate to shifts in chemical bond energies as shown in previous work[21,23,24]. Fig. 5 shows XPS spectra from two graphite samples exposed via the PMI probe to NSTX lithium conditioned NB heated plasmas. Pane (a) show XPS spectra after 15m of Ar cleaning of a graphite sample that was exposed to 6 NB heated plasmas and simultaneously, 63 nm Li deposition. Pane (b) shows XPS spectra after 15m (red curve) and 45 min (blue curve) of Ar cleaning from a graphite sample exposed to 40 NB plasmas and 817 nm of Li deposition. The amount of Li deposited is measured by a quartz microbalance at the same major radius, but toroidally displaced and the nominal thickness is calculated for a lithium density of 0.53 g/cm^3 on a flat surface. It can be seen that the peak at 532 eV shifts toward the Li-D-O peak at 533 eV with increasing lithium dose. More details associated with these peak shifts may be found in ref. [21,23,24].

Thermal desorption spectra (TDS) were obtained a few hours after plasma exposure withdrawing the samples to a chamber underneath NSTX and heating one of them with a controlled temperature ramp while measuring hydrocarbon emission with a calibrated quadrupole mass

spectrometer. These were followed by more controlled TDS measurements at Purdue. Fig. 6 shows a comparison of Purdue TDS spectra of 6 NB heated discharges before and with Li-conditioning. The TDS data is plotted as the partial pressure of all deuterium atoms desorbed by heating the sample to temperatures above 800 K. The data shows two peaks corresponding to effective release of deuterium. The peak near 600 K indicates a weakly bonding state for D atoms to C or O in the presence of lithium. Higher peaks indicate stronger covalent/ionic bonding to Li, O, and/or C. This observation appears to be consistent with global retention measurements in NSTX with evidence of prompt D release. TDS data show that the primary release channel is 20 amu corresponding predominantly to D₂O when heated. Samples exposed to ohmically heated plasmas showed 19 and 31 amu as primary release channel corresponding to C_xD₃H. The difference between OH and NB shots will be investigated by extending the TDS to temperatures above 1000 K. However, the *total* D emission at 600K is the same for both cases.

4. Conclusions.

In summary, the end of pulse deuterium retention is high (~ 90%) and attributed mostly to wall pumping over the relatively short NSTX pulse duration and to the minimal wall heating achieved with the controlled ramp down. The retention increased slightly with lithium conditioning, the difference being more noticeable with heavy lithium conditioning. XPS analysis of graphite samples exposed to these plasmas showed peaks that were previously identified with chemical functionalities associated with deuterium irradiation of a graphite surface conditioned with lithium. There is an interesting correlation of dependence of the XPS peaks on lithium deposition and the increased difference in D retention with increased Li deposition shown in the retention results in Table 1. We note however that the lithium-induced suppression of ELMs may also contribute to the change in retention in NB heated discharges. The additional deuterium retained with lithium was released promptly after the discharge. This may be understood in the light of the low energy D bonding peak revealed by TDS analysis of lithium-conditioned samples. The small difference in global retention from gas-balance results yet large effects from lithium conditioning on plasma performance indicate the importance of the *dynamic* “coupling” between the edge plasma and the material interface. More work is needed to unravel the *dynamic* nature of D retention on promptly deposited lithium coatings in NSTX. This can be addressed with future efforts in expanding *in-situ* PMI diagnostics that can probe plasma-exposed surface during

or shortly-after irradiation to elucidate on the fundamental mechanisms that dictate D recycling at the plasma-material interface.

Acknowledgements.

The authors thank R. Raman, T Holoman, D LaBrie, and the NSTX team. Support is provided by the U.S. DOE Contract Nos. DE AC02-09CH11466, DE-FG02-08ER54990 DE-AC05-00OR22725 and DE-AC52-07NA27344.

Figure Captions:

Fig. 1 (a) Plasma current, (b) stored energy and (c) in-vessel pressure for gas-only 'shot' (thin line) and ohmic discharge (thick line) with lithium conditioning.

Fig. 2 (a) Plasma current, (b) stored energy and (c) in-vessel pressure for gas-only 'shot' (thin line) and NB heated discharge (thick line) before lithium conditioning. The gas fueling was programmed to be the same in both cases. The NB power is shown dashed.

Fig. 3 (a) plasma current, (b) stored energy (c) in-vessel pressure and (d) wall inventory calculated by dynamic particle balance model for pre-Li (thin line) and with-Li (thick line) NB heated discharges.

Fig. 4 Probe configuration on the lower NSTX vessel with magnetic flux lines for a low triangularity plasma. The chamber has been rotated 90° to show: (a) port for residual gas analyser or sample insertion, (b) pumping port, (c) probe drive and (d) probe head. An image of the probe head with 4 samples is shown in insert (e).

Fig. 5 XPS O1s spectra from two graphite samples showing 533.0 eV peak associated with retention of D in lithiated graphite matrix. PMI Probe sample ATJ 150p (lower pane) has about 10 more times lithium deposition than sample ATJ 139p (upper pane). The thin lines represent multiple peaks that compose the primary peak. The dashed lines are the spectra before Ar cleaning.

Fig. 6. Thermal desorption spectra (TDS) of ATJ graphite samples exposed via the PMI probe to 6 NB heated NSTX discharges with-, (a), and without-, (b), lithium exposure. The mass=20 peak is plotted separately and corresponds to emission of D₂O.

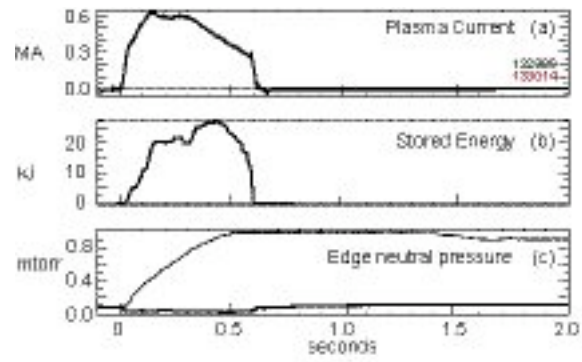


Fig. 1 (a) Plasma current, (b) stored energy and (c) in-vessel pressure for gas-only 'shot' (thin line) and ohmic discharge (thick line) with lithium conditioning.

C.H. Skinner et al. JNM Fig. 1

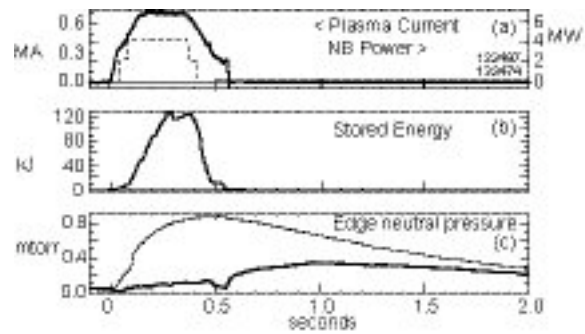


Fig. 2 (a) Plasma current, (b) stored energy and (c) in-vessel pressure for gas-only 'shot' (thin line) and neutral beam heated discharge (thick line) before lithium conditioning. The gas fueling was programmed to be the same in both cases. The neutral beam power is shown dashed.

C.H. Skinner et al. JNM Fig. 2

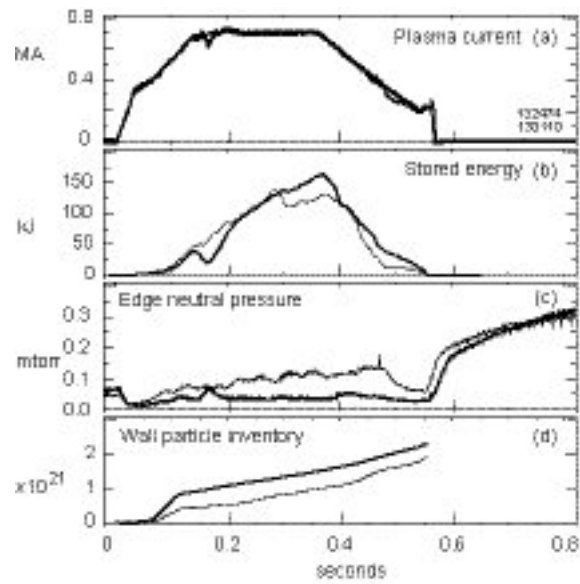


Fig. 3 (a) plasma current, (b) stored energy (c) in-vessel pressure and (d) wall inventory calculated by dynamic particle balance model for pre-Li (thin line) and with-Li (thick line) neutral beam heated discharges.

C.H. Skinner et al. JNM Fig. 3

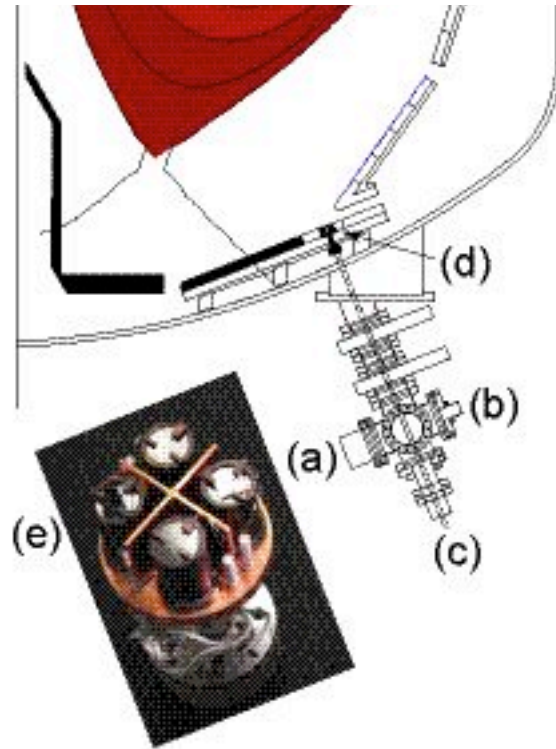


Fig. 4 Probe configuration on the lower NSTX vessel with magnetic flux lines for a low triangularity plasma. The chamber has been rotated 90° to show: (a) port for residual gas analyser or sample insertion, (b) pumping port, (c) probe drive and (d) probe head. An image of the probe head with 4 samples is shown in insert (e).

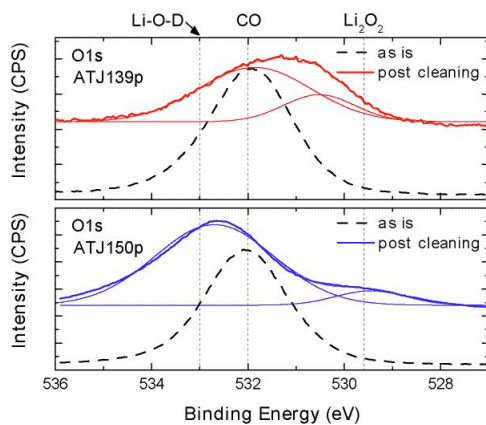


Fig. 5 XPS O1s spectra from two graphite samples showing 533.0 eV peak associated with retention of D in lithiated graphite matrix. PMI Probe sample ATJ 150p (lower pane) has about 10 more times lithium deposition than sample ATJ 139p (upper pane). The thin lines represent multiple peaks that compose the primary peak. The dashed lines are the spectra before Ar cleaning.

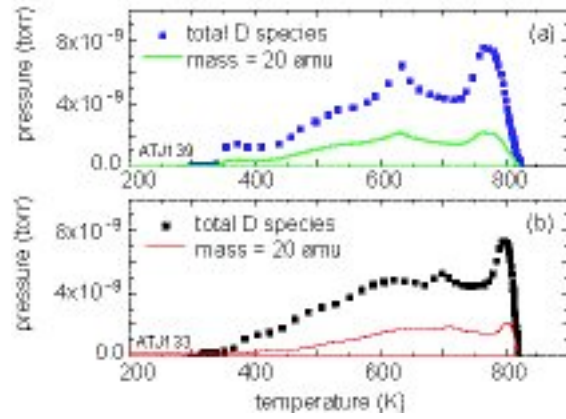


Fig. 6. Thermal desorption spectra (TDS) of ATJ graphite samples exposed via the PMI probe to 6 NB heated NSTX discharges with-, (a), and without-, (b), lithium exposure. The mass=20 peak is plotted separately and corresponds to emission of D_2O .

References

- [1] H. Bergsaker, et al., J. Nucl. Mater., 145-147 (1987) 727.
- [2] W. R. Wampler, B. L. Doyle, and A. E. Pontau, J. Nucl. Mater., 145-147 (1987) 353.
- [3] T Loarer, J. Nucl. Mater., 390-391 (2009) 20.
- [4] G. Haas et al., J. Nucl. Mater., 266-269 (1999) 1065
- [5] C. H. Skinner et al., J. Nucl. Mater., 363-365 (2007) 247.
- [6] T. Loarer et al., Nucl. Fus 47 (2009) 1112.
- [7] V. Rohde et al., Nucl. Fusion 49 (2009) 085031
- [8] C.H. Skinner, et al., Fus. Sci. Technol. **54** (2008) 891.
- [9] D. K. Mansfield et al., Phys. Plasmas 3 (1996) 1892.
- [10] S. V. Mirnov et al., Plasma Phys. Control. Fusion 48 (2006) 821.
- [11] M. L. Apicella et al., Journal of Nuclear Materials 386–388 (2009) 821.
- [12] R. Kaita et al., Phys. Plasmas 14, (2007) 056111,.
- [13] J. Sanchez et al., Nucl. Fus. 49 (2009) 104018.
- [14] R. Majeski et al., Nucl. Fusion 49, (2009) 055014.
- [15] H. W. Kugel et al., J. Nucl. Mater., 390-391 (2009) 1000.
- [16] M. Bell et al., Plasma Phys. Contr. F. 51 (2009) 124054
- [17] H. W. Kugel et al., this proceedings.
- [18] L. E. Zakharov, Fus. Eng. and Design, 72 (2004) 149.
- [19] M. J. Baldwin et al., Nucl Fusion 42, (2002) 1318
- [20] S. Kato et al., J. Nucl. Mater., 266 (1999) 406
- [21] J. P. Allain et al., J. Nucl. Mater., 390-91(2009) 942
- [22] H. Yagi et al., J. Nucl. Mater., 313–316 (2003) 284.
- [23] S. S. Harilal et al., Appl. Surf. Sci., 255, (2009) 8539.
- [24] C.N. Taylor et al, these proceedings
- [25] V. Soukhanovski et al., J. Nucl. Mater., 390-391 (2009) 516.
- [26] V.A. Soukhanovskii et al., J. Nucl. Mater., 313-316 (2003) 73.

[27] R. Maingi et al., Nucl. Fus., 36 (1996) 245.

The Princeton Plasma Physics Laboratory is operated
by Princeton University under contract
with the U.S. Department of Energy.

Information Services
Princeton Plasma Physics Laboratory
P.O. Box 451
Princeton, NJ 08543

Phone: 609-243-2245
Fax: 609-243-2751
e-mail: pppl_info@pppl.gov
Internet Address: <http://www.pppl.gov>